Geophys. J. R. astr. Soc. (1977) **48**, 493–508

Solution of the *H*-polarization induction problem by a wavenumber integral equation approach

K. Sørensen and L. Børsting Pedersen *Laboratory of Geophysics, University of Aarhus, Denmark, Finlandsgade 6–8, DK-8200, Aarhus N*

Received 1976 July 7; in original form 1976 February 9

Summary. The *H*-polarization induction problem is solved in terms of an integral equation, which in the horizontal direction is transformed into the wavenumber domain. By this transformation the usual complicated integral expressions for the Green's tensor elements are removed. By extracting asymptotic features from the system of linear equations, we reduce the number of equations considerably independent of whether the horizontal variation in the conductivity is continuous or discontinuous. Likewise we reformulate the problem so that arbitrary conductivity contrasts may be studied. The method is finally tested by comparing with analytic solutions, and good agreement is achieved. Furthermore the numerical results indicate that a small amount of wavenumbers is required.

1 Introduction

It is well-known that the electromagnetic field equations in the magnetotelluric case separate into *H*- and *E*-polarization, if the structure is two-dimensional (Porstendorfer 1975; Hobbs 1975).

Many attempts have been made to solve the equations connected to these two polarizations. One way is to focus on the differential equation and solve it by means of a finite element or finite difference technique (Jones & Pascoe 1071; Coggon 1971; Reddy & Rankin 1973); another is to transform the differential equation into an integral equation using a Green's function formalism (Hohmann 1971; Raiche 1974; Weidelt 1975a). The advantage of the last method is that the area in which the equation has to be solved is reduced to the anomalous area. But the disadvantage is that it turns out to be very time consuming to compute the Fourier integral expressing the Green's function.

Therefore, an attempt has been made to solve the equations in the Fourier space, because such a transformation removes the Fourier integral connected to the Green's function. Another advantage of the present method is that it becomes quite easy to treat continuous conductivity changes, which are difficult to handle by the above mentioned methods. SI-units are used.

2 Derivation of the integral equation

If the source field is a plane wave and the structure is two-dimensional (the x-direction being the independent direction), then the field equations separate into two independent systems. We shall assume that the frequencies used are below that level where displacement currents have to be taken into account. The time dependence is described by $\exp(i\omega t)$. Under the assumptions mentioned above Maxwell's equations become

$$\text{curl}\,\mathbf{H}(\mathbf{r}) = \sigma(\mathbf{r})\,\mathbf{E}(\mathbf{r}) + \mathbf{j}_e(\mathbf{r})$$

$$\text{curl}\,\mathbf{E}(\mathbf{r}) = -i\omega\mu_0\,\mathbf{H}(\mathbf{r})$$

or combined

$$\text{curl}^2\,\mathbf{E}(\mathbf{r}) + k^2(\mathbf{r})\,\mathbf{E}(\mathbf{r}) = -i\omega\mu_0\,\mathbf{j}_e(\mathbf{r})$$

where in the case of H-polarization

$$\mathbf{H} = (H_x, 0, 0)$$

$$\mathbf{E} = (0, E_y, E_z)$$

$$k^2(\mathbf{r}) = i\omega\mu_0\,\sigma(\mathbf{r})$$

$\sigma(\mathbf{r})$ is the conductivity, which is assumed to be zero in the air halfspace and non-zero in the earth halfspace. $\mathbf{j}_e = \hat{\mathbf{x}}_y j_0 \delta(z+h)$ due to a uniform current sheet at height $z = -h\,(h > 0)$. This assumption, however, is immaterial for the following.

Referring to Weidelt (1975a) we obtain

$$\mathbf{E}_a(\mathbf{r}_0) = \int k_a^2(\mathbf{r})\,\mathbf{G}(\mathbf{r}_0|\mathbf{r})\,\mathbf{E}(\mathbf{r})\,dA \tag{1}$$

where

$$\text{curl}^2\,\mathbf{E}_n(\mathbf{r}) + k_n^2(\mathbf{r})\,\mathbf{E}_n(\mathbf{r}) = -i\omega\mu_0\,\mathbf{j}_e(\mathbf{r});$$

$$\mathbf{G}(\mathbf{r}_0|\mathbf{r}) = \hat{\mathbf{x}}_y\,\mathbf{G}_y(\mathbf{r}_0|\mathbf{r}) + \hat{\mathbf{x}}_z\,\mathbf{G}_z(\mathbf{r}_0|\mathbf{r})$$

$$= \hat{\mathbf{x}}_y\hat{\mathbf{x}}_y\,G_{yy} + \hat{\mathbf{x}}_y\hat{\mathbf{x}}_z G_{yz} + \hat{\mathbf{x}}_z\hat{\mathbf{x}}_y\,G_{zy} + \hat{\mathbf{x}}_z\hat{\mathbf{x}}_z\,G_{zz}; \qquad \text{using dyadic notation}$$

$$\text{curl}^2\,\mathbf{G}_i(\mathbf{r}_0|\mathbf{r}) + k_n^2(\mathbf{r})\,\mathbf{G}_i(\mathbf{r}_0|\mathbf{r}) = -\hat{\mathbf{x}}_i\,\delta(\mathbf{r}-\mathbf{r}_0); \qquad i = y, z \tag{2}$$

with

$$k^2(\mathbf{r}) = k_n^2(\mathbf{r}) + k_a^2(\mathbf{r})$$

$k_n^2(\mathbf{r})$ refers to the normal part of the model, consisting of a set of horizontal uniform layers, and $k_a^2(\mathbf{r})$ refers to the anomalous part.

The tensor element $G_{ij}(\mathbf{r}_0|\mathbf{r})$ has a simple physical interpretation: $G_{ij}(\mathbf{r}_0|\mathbf{r})$ is the jth electric field component at $\mathbf{r}$ of an infinite row in the x-direction of oscillating electric dipoles of unit moment in the $\hat{\mathbf{x}}_i$ direction at $\mathbf{r}_0$.

3 Computation of the Green's tensor

We now consider a normal conductivity structure consisting of a non-conducting air halfspace (index 0) and M uniform conducting layers with conductivities σ_m, $m = 1, 2, \ldots, M$. In order to calculate the Green's tensor, two infinite rows in the x-direction of oscillating

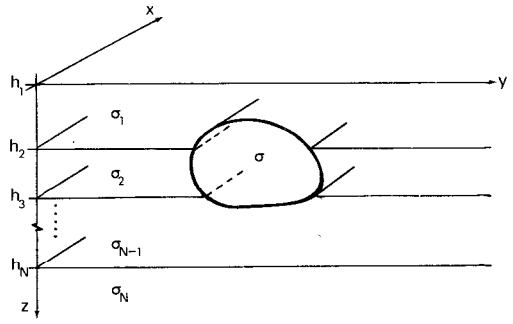

Figure 1. The general two-dimensional model.

electric dipoles pointing in the y-direction and z-direction, respectively, are placed at $\mathbf{r}_0$ and the resulting field from each row is calculated at $\mathbf{r}$.

Let the dipole row with moments in the $\hat{\mathbf{x}}_i$ direction be placed in the μth layer at $\mathbf{r}_0$. Then $\mathbf{G}_i^m(\mathbf{r}_0 \mid \mathbf{r})$ is the resulting field in the mth layer at $\mathbf{r}$. The continuity of the tangential components of the electrical and magnetic fields at interfaces leads to the conditions

$$\begin{aligned} &\hat{z} \times (\mathbf{G}_i^{m-1} - \mathbf{G}_i^m) = 0; \\ &\hat{z} \times \operatorname{curl}(\mathbf{G}_i^{m-1} - \mathbf{G}_i^m) = 0; \\ &z = h_m, \; m = 1, \ldots, M. \end{aligned} \tag{3}$$

Now define

$$\operatorname{curl} \mathbf{G}_i^m(\mathbf{r}_0 \mid \mathbf{r}) = \mathbf{S}_i^m(\mathbf{r}_0 \mid \mathbf{r}) = (S_{ix}^m(\mathbf{r}_0 \mid \mathbf{r}), 0, 0) \tag{4}$$

$$\operatorname{curl} \mathbf{S}_i^m(\mathbf{r}_0 \mid \mathbf{r}) = -k_m^2 \mathbf{G}_i^m(\mathbf{r}_0 \mid \mathbf{r}) - \hat{x}_i \delta(\mathbf{r} - \mathbf{r}_0) \tag{5}$$

where $i = y, z$, $k_m^2 = i\omega\mu_0\sigma_m$.

Combining equations (4) and (5) and using $\operatorname{div} \mathbf{S}_i^m(\mathbf{r}_0 \mid \mathbf{r}) = 0$

$$\Delta S_{yx}^m(\mathbf{r}_0 \mid \mathbf{r}) - k_m^2 S_{yx}^m(\mathbf{r}_0 \mid \mathbf{r}) = -\delta(y - y_0) \frac{\partial}{\partial z} \delta(z - z_0) \tag{6}$$

$$\Delta S_{zx}^m(\mathbf{r}_0 \mid \mathbf{r}) - k_m^2 S_{zx}^m(\mathbf{r}_0 \mid \mathbf{r}) = \delta(z - z_0) \frac{\partial}{\partial y} \delta(y - y_0). \tag{7}$$

The equations of continuity of $\mathbf{S}_i^m$ are obtained from (3), (4), and (5)

$$S_{ix}^m(\mathbf{r}_0 \mid \mathbf{r}) = S_{ix}^{m+1}(\mathbf{r}_0 \mid \mathbf{r}) \tag{8}$$

$$\frac{1}{\sigma_m} \frac{\partial}{\partial z} S_{ix}^m(\mathbf{r}_0 \mid \mathbf{r}) = \frac{1}{\sigma_{m+1}} \frac{\partial}{\partial z} S_{ix}^{m+1}(\mathbf{r}_0 \mid \mathbf{r}) \tag{9}$$

where $\mathbf{r} = (y, h_{m+1})$ and $i = y, z$.

In order to solve (6) and (7) we consider the following equation

$$\Delta g_i^m(\mathbf{r}_0 \mid \mathbf{r}) - k_m^2 g_i^m(\mathbf{r}_0 \mid \mathbf{r}) = -\delta(\mathbf{r} - \mathbf{r}_0) \tag{10}$$

with

$$S_{yx}^m(\mathbf{r}_0 \mid \mathbf{r}) = \frac{\partial}{\partial z} g_y^m(\mathbf{r}_0 \mid \mathbf{r}) \tag{11}$$

$$S^m_{zx}(\mathbf{r}_0|\mathbf{r}) = -\frac{\partial}{\partial y} g^m_z(\mathbf{r}_0|\mathbf{r}). \tag{12}$$

Finally, using (4), (5), and (12) the succeeding expressions are achieved for the Green's tensor

$$G^m_{yy}(\mathbf{r}_0|\mathbf{r}) = \frac{1}{k_m^2}\left[\frac{\partial^2}{\partial y^2} - k_m^2\right] g^m_y(\mathbf{r}_0|\mathbf{r})$$

$$G^m_{yz}(\mathbf{r}_0|\mathbf{r}) = \frac{1}{k_m^2}\frac{\partial}{\partial y}\frac{\partial}{\partial z} g^m_y(\mathbf{r}_0|\mathbf{r})$$

$$G^m_{zz}(\mathbf{r}_0|\mathbf{r}) = \frac{1}{k_m^2}\left[\frac{\partial^2}{\partial z^2} - k_m^2\right] g^m_z(\mathbf{r}_0|\mathbf{r})$$

$$G^m_{zy}(\mathbf{r}_0|\mathbf{r}) = \frac{1}{k_m^2}\frac{\partial^2}{\partial y\,\partial z} g^m_z(\mathbf{r}_0|\mathbf{r}).$$

Equation (10) is solved by using the procedure introduced by Weidelt (1975b) with the following continuity conditions as implied by (8) and (9)

$$\frac{\partial}{\partial z} g^m_y(\mathbf{r}_0|\mathbf{r}) = \frac{\partial}{\partial z} g^{m+1}_y(\mathbf{r}_0|\mathbf{r}) \tag{13}$$

$$\frac{1}{\sigma_m}\frac{\partial^2}{\partial z^2} g^m_y(\mathbf{r}_0|\mathbf{r}) = \frac{1}{\sigma_{m+1}}\frac{\partial^2}{\partial z^2} g^{m+1}_y(\mathbf{r}_0|\mathbf{r}) \tag{14}$$

$$g^m_z(\mathbf{r}_0|\mathbf{r}) = g^{m+1}_z(\mathbf{r}_0|\mathbf{r}) \tag{15}$$

$$\frac{1}{\sigma_m}\frac{\partial}{\partial z} g^m_z(\mathbf{r}_0|\mathbf{r}) = \frac{1}{\sigma_{m+1}}\frac{\partial}{\partial z} g^{m+1}_z(\mathbf{r}_0|\mathbf{r}) \tag{16}$$

$\mathbf{r} = (y, h_{m+1})$.

The functions $g^m_y(\mathbf{r}_0|\mathbf{r})$ and $g^m_z(\mathbf{r}_0|\mathbf{r})$ are expressed by a Fourier integral along the y-direction. By assuming that $\delta(\mathbf{r} - \mathbf{r}_0) = 0$ in the air halfspace, i.e. the anomalous domain is confined to lie within the Earth, it is immediately obtained from (5) that $S^0_{yx}(\mathbf{r}_0|\mathbf{r})$ and $S^0_{zx}(\mathbf{r}_0|\mathbf{r})$ are constants for $z < 0$. The constants are equal to zero due to (4), because $\mathbf{G}^0_i$ vanishes at $z = -\infty$

$$\begin{aligned} &S^0_{yx}(\mathbf{r}_0|\mathbf{r}) = 0 \\ &\qquad z \leqslant 0 \text{ (air halfspace)} \\ &S^0_{zx}(\mathbf{r}_0|\mathbf{r}) = 0 \end{aligned} \tag{17}$$

$g^m_y(\mathbf{r}_0|\mathbf{r})$ is considered first

$$g^m_y(\mathbf{r}_0|\mathbf{r}) = \int_0^\infty [R^+_m + R^-_m] \cos[2\pi\lambda(y - y_0)]\, d\lambda$$

where

$$R_m^{\pm} = \begin{cases} \pm\gamma_0 \dfrac{K_m^{\pm}}{\alpha_m} f_m^{\pm} & z_0 \geqslant z \\ \pm\gamma_L \dfrac{L_m^{\pm}}{\alpha_m} f_m^{\pm} & z > z_0 \end{cases}$$

$f_m^{\pm} = \exp[\pm\alpha_m(z - h_m)]$

$\alpha_m = [k_m^2 + (2\pi\lambda)^2]^{1/2}$.

From (11) and (17) it is obtained that $K_1^+ + K_1^- = 0$, and the solution $K_1^+ = 1$ and $K_1^- = -1$ is used. In order to get finite solutions at $z = \infty$, it is required that $L_M^+ = 0$, and we choose $L_M^- = 1$. The continuity conditions equations (13) and (14) imply the recursion formulae

$$K_m^{\pm} = \tfrac{1}{2}\left[K_{m-1}^+ g_{m-1}^+ \left(1 \pm \frac{\alpha_{m-1}\sigma_m}{\alpha_m \sigma_{m-1}}\right) + K_{m-1}^- g_{m-1}^- \left(1 \mp \frac{\alpha_{m-1}\sigma_m}{\alpha_m \sigma_{m-1}}\right)\right], \quad \mu \geqslant m \geqslant 2$$

$$L_m^{\pm} = \tfrac{1}{2} g_m^{\mp}\left[L_{m+1}^+ \left(1 \pm \frac{\alpha_{m+1}\sigma_m}{\alpha_m \sigma_{m+1}}\right) + L_{m+1}^- \left(1 \mp \frac{\alpha_{m+1}\sigma_m}{\alpha_m \sigma_{m+1}}\right)\right], \quad M - 1 \geqslant m \geqslant \mu$$

with $g_m^{\pm} = \exp[\pm\alpha_m(h_{m+1} - h_m)]$.

The constants γ_0 and γ_L are determined from adjustment of upgoing and downgoing waves at $z = z_0$ which is assumed to be in the μth layer

$$\gamma_L = \frac{K_\mu^- f_\mu^- - K_\mu^+ f_\mu^+}{L_\mu^- K_\mu^+ - L_\mu^+ K_\mu^-}$$

$$\gamma_0 = \frac{L_\mu^- f_\mu^- - L_\mu^+ f_\mu^+}{L_\mu^- K_\mu^+ - L_\mu^+ K_\mu^-}, \quad f_\mu^{\pm} = (f_\mu^{\pm})_{z=z_0}$$

$g_z^m(\mathbf{r}_0 \mid \mathbf{r})$ is treated in a similar manner

$$g_z^m(\mathbf{r}_0 \mid \mathbf{r}) = \int_0^{\infty} [Q_m^+ + Q_m^-] \cos 2\pi\lambda(y - y_0)\, d\lambda$$

$$Q_m^{\pm} = \begin{cases} \delta_0 C_m^{\pm} f_m^{\pm} & z_0 \geqslant z \\ \delta_L D_m^{\pm} f_m^{\pm} & z > z_0. \end{cases}$$

Again we choose

$C_1^+ = 1$, $C_1^- = -1$, $D_M^- = 1$, $D_M^+ = 0$.

The continuity conditions equations (15) and (16) imply the recursion formulae

$$C_m^{\pm} = \tfrac{1}{2}\left[C_{m-1}^+ g_{m-1}^+ \left(1 \pm \frac{\alpha_{m-1}\sigma_m}{\alpha_m \sigma_{m-1}}\right) + C_{m-1}^- g_{m-1}^- \left(1 \mp \frac{\alpha_{m-1}\sigma_m}{\alpha_m \sigma_{m-1}}\right)\right], \quad \mu \geqslant m \geqslant 2$$

$$D_m^{\pm} = \tfrac{1}{2} g_m^{\mp}\left[D_{m+1}^+ \left(1 \pm \frac{\alpha_{m+1}\sigma_m}{\alpha_m \sigma_{m+1}}\right) + D_{m+1}^- \left(1 \mp \frac{\alpha_{m+1}\sigma_m}{\alpha_m \sigma_{m+1}}\right)\right], \quad M - 1 \geqslant m \geqslant \mu.$$

The constants δ_0 and δ_L are again determined from adjustment of upgoing and downgoing waves at $z = z_0$ (μth layer)

$$\delta_L = \frac{1}{\alpha_\mu} \frac{C_\mu^+ f_\mu^+ + C_\mu^- f_\mu^-}{D_\mu^- C_\mu^+ - D_\mu^+ C_\mu^-}$$

$$\delta_0 = \frac{1}{\alpha_\mu} \frac{D_\mu^+ f_\mu^+ + D_\mu^- f_\mu^-}{D_\mu^- C_\mu^+ - D_\mu^+ C_\mu^-}, \quad f_\mu^\pm = (f_\mu^\pm)_{z=z_0}.$$

The reason for the difference in the definitions of $R_m^\pm$ and $Q_m^\pm$ is that the same recursion formulae are achieved. This is, of course, a computational advantage.

Defining

$$F_{yy}^m(\lambda, z_0, z) = -\frac{1}{2k_m^2} \alpha_m^2 [R_m^+ + R_m^-]$$

$$F_{yz}^m(\lambda, z_0, z) = -\frac{1}{2ik_m^2} \alpha_m 2\pi\lambda [R_m^+ - R_m^-]$$

$$F_{zz}^m(\lambda, z_0, z) = \frac{1}{2k_m^2} (2\pi\lambda)^2 [Q_m^+ + Q_m^-]$$

$$F_{zy}^m(\lambda, z_0, z) = -\frac{1}{2ik_m^2} \alpha_m 2\pi\lambda [Q_m^+ - Q_m^-].$$

The following expressions for the Green's tensor are achieved (dropping indices m)

$$\mathbf{G}(\mathbf{r}_0 | \mathbf{r}) = \int_{-\infty}^{\infty} \mathbf{F}(\lambda, z_0, z) \exp [i2\pi\lambda(y - y_0)] \, d\lambda$$

$$\mathbf{F} = \hat{\mathbf{x}}_y \hat{\mathbf{x}}_y F_{yy} + \hat{\mathbf{x}}_y \hat{\mathbf{x}}_z F_{yz} + \hat{\mathbf{x}}_z \hat{\mathbf{x}}_y F_{zy} + \hat{\mathbf{x}}_z \hat{\mathbf{x}}_z F_{zz}. \tag{18}$$

The reciprocity relationship between source and receiver

$G_{ij}(\mathbf{r}_0 | \mathbf{r}) = G_{ji}(\mathbf{r} | \mathbf{r}_0)$

(Weidelt 1975a) implies that

$F_{yy}(\lambda, z_0, z) = F_{yy}(\lambda, z, z_0)$

$F_{yz}(\lambda, z_0, z) = -F_{zy}(\lambda, z, z_0)$

$F_{zz}(\lambda, z_0, z) = F_{zz}(\lambda, z, z_0).$

4 Fourier transformation of the integral equation

The integral equation (1) has to be solved numerically, because an analytical solution has not been found as yet! This implies an approximation of the E-field. The most simple way to do this is to divide the anomalous domain into a grid and assume the E-field to be constant within each cell (Hohmann 1971; Weidelt 1975a). This may, of course, be a very coarse approximation and a better solution can be obtained by using the method of moments introduced by Harrington (1968) and applied by La Joie (1973).

The above mentioned methods for solving the integral equation all involve lengthy

numerical computations of Green's tensors, even if the filter method introduded by Ghosh (1971) is used.

In the present method a Fourier transformation of the integral equation (1) is made in order to avoid the integral expression (18). Introduce (18) in (1)

$$\mathbf{E}_a(y_0, z_0) = \int k_a^2(y, z) \int \mathbf{F}(\lambda, z_0, z) \exp[i2\pi\lambda(y - y_0)]\, d\lambda\, \mathbf{E}(y, z)\, dy\, dz \tag{19}$$

Now define

$$\mathbf{E}_a(y, z) = \int_{-\infty}^{\infty} \hat{\mathbf{E}}(\lambda, z) \exp(-i2\pi\lambda y)\, d\lambda$$

$$\mathbf{E}_n(z) = \int_{-\infty}^{\infty} \mathbf{E}_n(z)\, \delta(\lambda) \exp(-i2\pi\lambda y)\, d\lambda$$

$$\delta(\lambda) = \int_{-\infty}^{\infty} \exp(i2\pi\lambda y)\, dy.$$

Using these definitions in (19) we get after some evaluations

$$\hat{\mathbf{E}}_a(\lambda, z_0) = \int \mathbf{F}(\lambda, z_0, z)\, \mathbf{E}_n(z)\, k_a^2(y, z) \exp(i2\pi\lambda y)\, dy\, dz$$

$$+ \iint_{-\infty}^{\infty} \mathbf{F}(\lambda, z_0, z)\, \hat{\mathbf{E}}_a(s, z)\, k_a^2(y, z) \exp(i2\pi(\lambda - s)y)\, ds\, dy\, dz. \tag{20}$$

In order to discretize the integration over s we first use the well-known interpolation theorem (Bracewell 1965, p. 189–197)

$$\hat{\mathbf{E}}_a(\lambda, z) = \sum_{-\infty}^{\infty} \hat{\mathbf{E}}_a\left(\frac{n}{2y_s}, z\right) \operatorname{sinc} 2y_s \left(\lambda - \frac{n}{2y_s}\right)$$

with

$$\operatorname{sinc} s = \frac{\sin \pi s}{\pi s}.$$

This interpolation is valid provided the spectrum of $\hat{\mathbf{E}}_a(\lambda, z_0)$ is bandlimited. The spectrum of $\hat{\mathbf{E}}_a(\lambda, z_0)$ is, of course, equal to $\mathbf{E}_a(y_0, z_0)$ and in some distance y_s we may assume

$$\mathbf{E}_a(y, z) = 0 \qquad |y| > y_s$$

$$k_a(y, z) = 0 \qquad |y| > y_s.$$

When the interpolation is introduced in (20) and $\lambda = m/2y_s$ we get

$$\hat{\mathbf{E}}_a(\nu_m, z_0) = \int \mathbf{F}(\nu_m, z_0, z)\, \mathbf{E}_n(z)\, k_a^2(y, z) \exp(i2\pi\nu_m y)\, dy\, dz$$

$$+ \iint_{-\infty}^{\infty} \mathbf{F}(\nu_m, z_0, z) \sum_{-\infty}^{\infty} \hat{\mathbf{E}}_a(\nu_n, z) \operatorname{sinc} 2y_s(s - \nu_n)$$

$$\times\, k_a^2(y, z) \exp(i2\pi(\nu_m - s)y)\, ds\, dy\, dz; \tag{21}$$

$$\nu_m = \frac{m}{2y_s}, \qquad \nu_n = \frac{n}{2y_s}.$$

Define

$$\hat{k}_a^2(\nu_m, z) = \int_{-\infty}^{\infty} k_a^2(y, z) \exp(i2\pi\nu_m y)\, dy. \tag{22}$$

From (21) and (22) we derive

$$\hat{\mathbf{E}}_a(\nu_m, z_0) = \int \mathbf{F}(\nu_m, z_0, z)\, \mathbf{E}_n(z)\, \hat{k}_a^2(\nu_m, z)\, dz$$

$$+ \int \mathbf{F}(\nu_m, z_0, z) \frac{1}{2y_s} \sum_n \hat{\mathbf{E}}_a(\nu_n, z)\, \hat{k}_a^2(\nu_m - \nu_n, z)\, dz. \tag{23}$$

Finally, the anomalous field is computed

$$\mathbf{E}_a(y, z) = \int \hat{\mathbf{E}}_a(\lambda, z) \exp(-i2\pi\lambda y)\, d\lambda$$

$$= \Pi\left(\frac{y}{2y_s}\right) \frac{1}{2y_s} \sum_n \hat{\mathbf{E}}_a(\nu_n, z) \exp(-i2\pi\nu_n y) \tag{24}$$

with

$$\Pi\left(\frac{y}{2y_s}\right) = \begin{cases} 1, & |y| \leqslant y_s \\ 0, & |y| > y_s. \end{cases}$$

5 Numerical solution of the Fourier equation

Equation (23) requires an integration in the z-direction which can be performed analytically under the assumption that $\hat{\mathbf{E}}_a(\nu_m, z)$, $\hat{k}_a^2(\nu_m, z)$ and $\mathbf{E}_n(z)$ are constant in each interval $z_i - dz/2 : z_i + dz/2$. This approximation can, of course, be improved by using the method of moments (Harrington 1968), but as we are interested primarily in the lateral variation of the field we shall not in the present context be further concerned about this aspect. With the above assumption we finally get from (23)

$$\hat{\mathbf{E}}_a(\nu_m, z_j) = \sum_i \Theta(\nu_m, z_j, z_i)\, \mathbf{E}_n(z_i)\, \hat{k}_a^2(\nu_m, z_i)$$

$$+ \sum_i \Theta(\nu_m, z_j, z_i) \frac{1}{2y_s} \sum_n \hat{\mathbf{E}}_a(\nu_n, z_i)\, \hat{k}_a^2(\nu_m - \nu_n, z_i) \tag{25}$$

where

$$\Theta(\nu_m, z_j, z_i) = \int_{z_i - dz/2}^{z_i + dz/2} \mathbf{F}(\nu_m, z_j, z)\, dz.$$

$\Theta(\nu_m, z_j, z_i)$ is easily obtained from analytical integration of $\mathbf{F}(\nu_m, z_j, z)$. From the expressions for $\Theta(\nu_m, z_j, z_i)$ we obtain when $|m| \to \infty$

$$\Theta_{yz}(\nu_m, z_j, z_i) = \Theta_{zy}(\nu_m, z_j, z_i) = 0$$

$$\Theta_{yy}(\nu_m, z_j, z_i) = -\frac{1}{k_n^2(z_j)}\,\delta_{ji} \tag{26}$$

$$\Theta_{zz}(\nu_m, z_j, z_i) = \frac{1}{k_n^2(z_j)}\,\delta_{ji}.$$

An approximate solution to (25) can be achieved from the following equation

$$\hat{\mathbf{E}}_a(\nu_m, z_j) = \sum_i \Theta(\nu_m, z_j, z_i)\,\mathbf{E}_n(z_i)\,\hat{k}_a^2(\nu_m, z_i)$$

$$+ \sum_i \Theta(\nu_m, z_j, z_i)\,\frac{1}{2y_s}\sum_{-N_c}^{N_c}\hat{\mathbf{E}}_a(\nu_n, z_i)\,\hat{k}_a^2(\nu_m - \nu_n, z_i) \tag{27}$$

N_c being a cutoff frequency.

6 Reformulation of the Fourier equation in order to get a better numerical scheme

As mentioned before, equation (23) must be solved numerically. This involves the choice of a cutoff frequency N_c. If $k_a^2(y, z)$ is a rapidly varying function of y, $\hat{k}_a^2(\nu_m - \nu_n, z_i)$ decays slowly as a function of $\nu_m - \nu_n$, and hence the approximation to the infinite summation in (23), i.e. the finite summation in (27) may be rather poor. In order to avoid this disadvantage we have developed a new equation for the numerical solution. From (19) we derive

$$\mathbf{E}_a(y_0, z_0) = \int k_a^2(y, z)\int \mathbf{F}(\lambda, z_0, z)\exp(i2\pi\lambda(y - y_0))\,d\lambda\,E_n(z)\,dy\,dz$$

$$+ \int k_a^2(y, z)\int [\mathbf{F}(\lambda, z_0, z) - \Theta^A(z_0, z)]\exp[i2\pi\lambda(y - y_0)]\,d\lambda$$

$$\times\,\mathbf{E}_a(y, z)\,dy\,dz + k_a^2(y_0, z_0)\,\Theta^A(z_0, z_0)\,\mathbf{E}_a(y_0, z_0). \tag{28}$$

The elements of Θ^A are the asymptotic values in (26). The reason for this manipulation is that the kernel $\mathbf{F}(\lambda, z_0, z)$ in the integral involving $\mathbf{E}_a(y, z)$ is replaced by a kernel $\mathbf{F}(\lambda, z_0, z) - \Theta^A(z_0, z)$ which decays to zero when $|\lambda| \to \infty$. Equation (28) implies that

$$k_a^2(y_0, z_0)\,\mathbf{E}_a(y_0, z_0) = k_a^2(y_0, z_0)\,[\mathbf{I} - k_a^2(y_0, z_0)\,\Theta^A(z_0, z_0)]^{-1}$$

$$\times \iint \mathbf{F}(\lambda, z_0, z)\exp[i2\pi\lambda(y - y_0)]\,d\lambda\,k_a^2(y, z)\,\mathbf{E}_n(z)\,dy\,dz$$

$$+ \iint [\mathbf{F}(\lambda, z_0, z) - \Theta^A(z_0, z)]\exp[i2\pi\lambda(y - y_0)]\,d\lambda\,k_a^2(y, z)$$

$$\times\,\mathbf{E}_a(y, z)\,dy\,dz.$$

The corresponding equation in the frequency domain is obtained by a Fourier transformation. Assuming the same approximations as for obtaining (25) we derive

$$\Gamma(\nu_m, z_j) = \sum_i \sum_n \beta(\nu_m - \nu_n, z_j)\, \Theta(\nu_n, z_j, z_i)\, \mathrm{E_n}(z_i)$$

$$+ \sum_i \sum_n \beta(\nu_m - \nu_n, z_j)\, [\Theta(\nu_n, z_j, z_i) - \Theta^{\mathrm{A}}(z_j, z_i)]\, \Gamma(\nu_n, z_i) \tag{29}$$

where

$$\beta(\nu_m - \nu_n, z_j) = \frac{1}{2y_s} \int_{-y_s}^{y_s} k_{\mathrm{a}}^2(y, z_j)\, [\mathbf{I} - k_{\mathrm{a}}^2(y, z_j)\, \Theta^{\mathrm{A}}(z_j, z_j)]^{-1} \times \exp[i2\pi(\nu_m - \nu_n) y]\, dy$$

$$\Gamma(\nu_n, z_i) = \frac{1}{2y_s} \sum_m \hat{\mathrm{E}}_{\mathrm{a}}(\nu_m, z_i)\, \hat{k}_{\mathrm{a}}^2(\nu_n - \nu_m, z_i); \quad \nu_m = \frac{m}{2y_s}.$$

Equation (29) is far more powerful when solving numerically because $\Theta(\nu_n, z_j, z_i) - \Theta^{\mathrm{A}}(z_j z_i)$ decays rapidly to zero when $|n| \to \infty$. Hence only a few terms in the summation involving $\Gamma(\nu_n, z_i)$ are necessary to get a good approximation for the sum. This implies that the linear system to solve for $\Gamma(\nu_n, z_i)$ is small.

7 A displacement technique for obtaining the numerical solution

Numerical experiments have shown that the convergence of the iteration process, based on equation (29), is strongly dependent on the ratio $\max[|\sigma_{\mathrm{a}}(y, z)|]/\sigma_{\mathrm{n}}(z)$. Only when this ratio is less than 1, the iteration converges for the tested examples. This means that models with a good conductor embedded in a bad conductor are difficult to treat. The problem can in most cases be solved using a spectrum displacement technique. We have developed a different method which seems to have a stronger effect because it reduces the norms of the eigenvalues of the coefficient matrix and makes it more diagonally dominant.

Consider the equation to be solved by the Green's tensor formalism (Weidelt 1975a)

$$\mathrm{curl}^2\, \mathbf{E}_{\mathrm{a}}(\mathbf{r}) + k_{\mathrm{n}}^2\, \mathbf{E}_{\mathrm{a}}(\mathbf{r}) = -k_{\mathrm{a}}^2 [\mathbf{E}_{\mathrm{a}}(\mathbf{r}) + \mathbf{E}_{\mathrm{n}}(\mathbf{r})] \tag{30}$$

k_{n}^2 is related to the layered structure and k_{a}^2 to the deviation from that part.

Now consider the following equation derived from (30)

$$\mathrm{curl}^2\, \mathbf{E}_{\mathrm{a}}(\mathbf{r}) + (k_{\mathrm{n}}^2 + k_{\mathrm{an}}^2)\, \mathbf{E}_{\mathrm{a}}(\mathbf{r}) = -k_{\mathrm{a}}^2 \mathbf{E}_{\mathrm{n}}(\mathbf{r}) - (k_{\mathrm{a}}^2 - k_{\mathrm{an}}^2)\, \mathbf{E}_{\mathrm{a}}(\mathbf{r}) \tag{31}$$

where $k_{\mathrm{an}}^2 = i\omega\mu_0\sigma_{\mathrm{an}}(z)$, $\sigma_{\mathrm{an}}(z)$ is y-independent, but otherwise arbitrary.

By means of the same techniques and approximations for obtaining (29) a similar equation can be found. But the convergence of the iteration process, based upon this equation, is strongly dependent on the ratio $\max[|\sigma_{\mathrm{a}}(y, z) - \sigma_{\mathrm{an}}(z)|]/[\sigma_{\mathrm{n}}(z) + \sigma_{\mathrm{an}}(z)]$. With a proper choice of $\sigma_{\mathrm{an}}(z)$ this ratio can be made less than 1. Furthermore the replacement of k_{n}^2 by $(k_{\mathrm{n}}^2 + k_{\mathrm{an}}^2)$ makes the coefficient matrix more diagonally dominant because the width of the corresponding Green's functions become smaller.

This displacement technique has been tested on models where good conductors are embedded in bad conductors and convergence of the iteration process was achieved even when large contrasts were considered [1 : (100–1000)].

8 Results

A FORTRAN program has been made and implemented on a CDC 6400 computer. Responses from different models are computed, and many of these models correspond to the one shown in Fig. 2. This model has the advantage that the *H*-polarization response can be evaluated analytically (Rankin 1962).

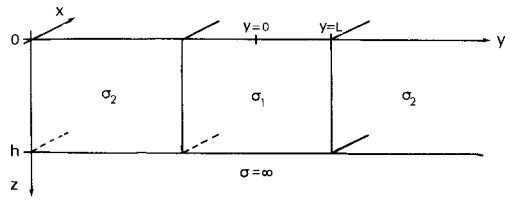

Figure 2. The model to which an analytical solution exists.

Let us consider Fig. 3, where the ρ_a-curve from the model in Fig. 2 is plotted for different y_s-values. y_s is the distance from the centre of the anomaly, where the anomalous field $\mathbf{E}_a$ is assumed to be zero. The shorter this distance becomes, the more pronounced the aliasing effect in the wavenumber domain will be. From Fig. 3 it is seen that saturation occurs at a distance of 1.5–2.0 km from the centre of the anomalous area. The reason why this saturation curve does not coincide with the analytical solution is that $\mathbf{E}_a$ is assumed to be constant in each slab of thickness 0.2 km. The penetration depth is 0.5 km so therefore this assumption is rather poor. In Fig. 4 y_s is equal to 1.5 km. In order to demonstrate the dependence of the cutoff frequency, curves with different numbers of coefficients are shown. The model is still the one shown in Fig. 2. Again a saturation occurs as the number of coefficients increases, and the asymptotic curve is reached around 10 coefficients, but a fairly good result is obtained with a smaller number, e.g. 6. In order to indicate the number of coefficients necessary to describe the response from a buried structure (Fig. 5), we refer to Fig. 6. Notice that the logarithmic scale is different from the scales used in Figs 3 and 4. Fig. 6 demonstrates that, in cases where a response from a buried structure is to be obtained, only a few coefficients are needed to reach a good agreement with the saturation curve. Of course, this was an expected result, because the response from a buried structure does not change abruptly and therefore needs a smaller number of coefficients to be described.

Figs 7 and 8 indicate that the responses from good conducting areas and bad conducting areas in the *H*-polarization case are of the same power. The model of these responses is given in Fig. 5.

Not much work has been carried out in connection with the investigation of the effect of continuous conductivity changes even if it is an important problem in relation to constructing realistic models for the interpretation of data. Therefore Fig. 9 shows the responses for different continuous conductivity changes. The model is the one described in Fig. 2, but the lateral anomalous conductivity change $\sigma_a = 5/(1 + (y/0.5)^{2p})$ is given by a continuous function. The function is chosen rather arbitrarily, but the responses show some interesting features. Even when $p = 24$, corresponding to nearly an abrupt change in σ_a at $y = 0.5$ km but the response does not coincide with the response from the model with the discontinuous change in conductivity.

9 Discussion and conclusions

The numerical results presented show both some of the advantages of the method and also they indicate some of the improvements that can be done.

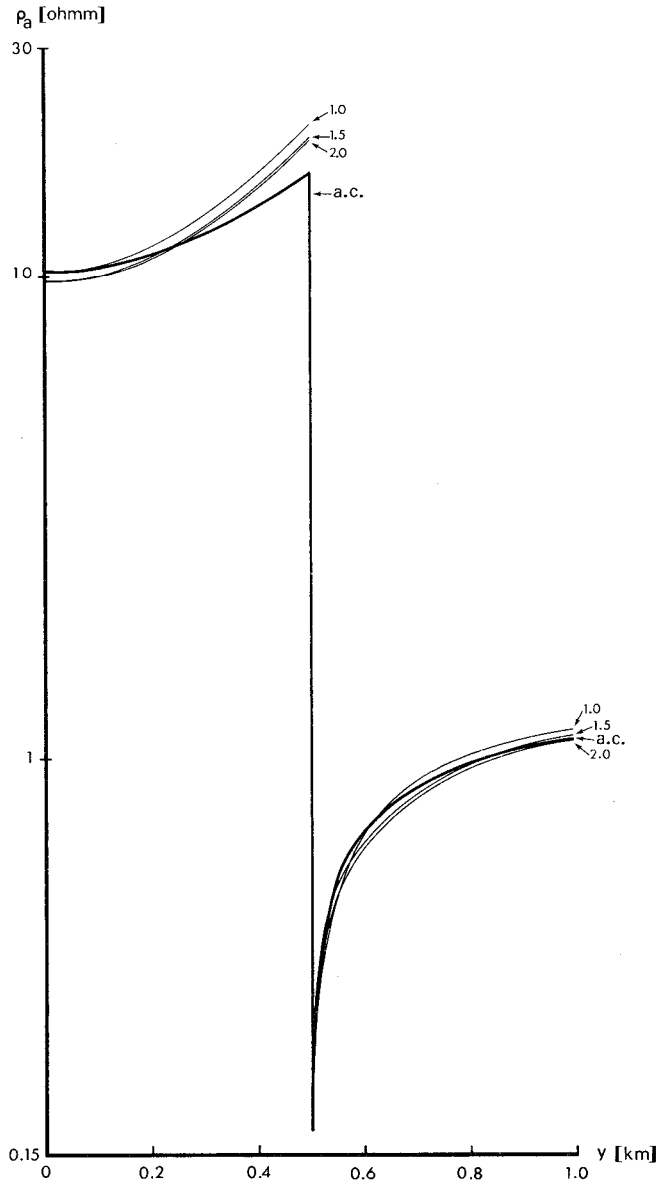

Figure 3. ρ_a-curves from the model Fig. 2. y_S = 1.0, 1.5, 2.0 km, $\omega = 2\pi$, ρ_1 = 10 ohmm, ρ_2 = 1 ohmm, L = 0.5 km, h = 1.0 km. The number of coefficients is 20; a.c. is the analytical solution.

It is interesting to note that good numerical results can be achieved by incorporating a few Fourier coefficients. Especially in relation to buried structures, this is pronounced. The result can be explained as a result of the exponential decay in the layered overburden of the high-frequency components of the anomalous field $\mathbf{E}_a$. Hence in such cases the system of linear equations to be solved will be small, which will cause the iteration process to converge rapidly. The accuracy of the method was studied by a comparison with analytical solutions, and good agreement was obtained, especially when remembering that the resolution in the z-direction was rather coarse. At this point it is worthwhile to point out that our zero order approximation, with $\mathbf{E}_a$ constant in each slab could be improved using, for example, a linear

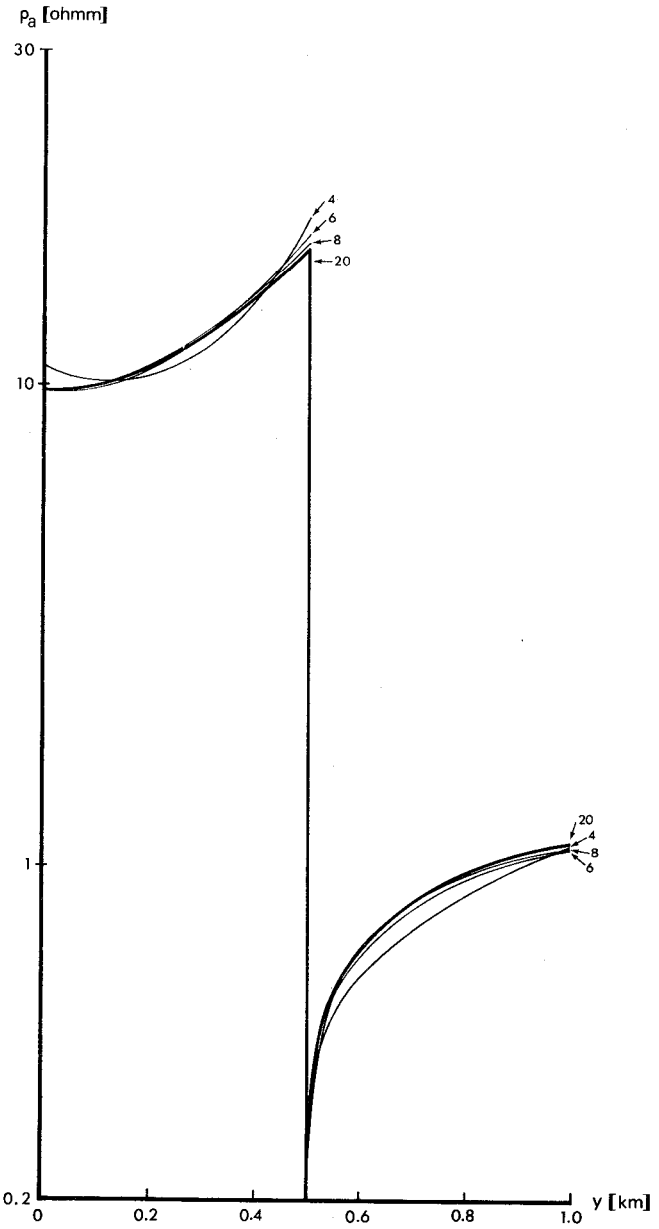

Figure 4. ρ_a-curves from the model Fig. 2. The number of coefficients is 4, 6, 8, 20. $\omega = 2\pi$, $\rho_1 = 10$ ohmm, $\rho_2 = 1$ ohmm, $L = 0.5$ km, $h = 1.0$ km, $y_s = 1.5$ km.

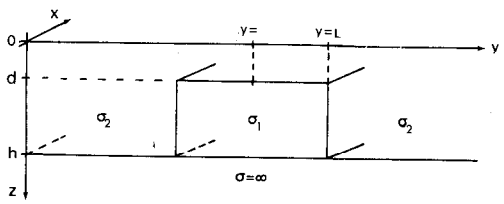

Figure 5. The buried model.

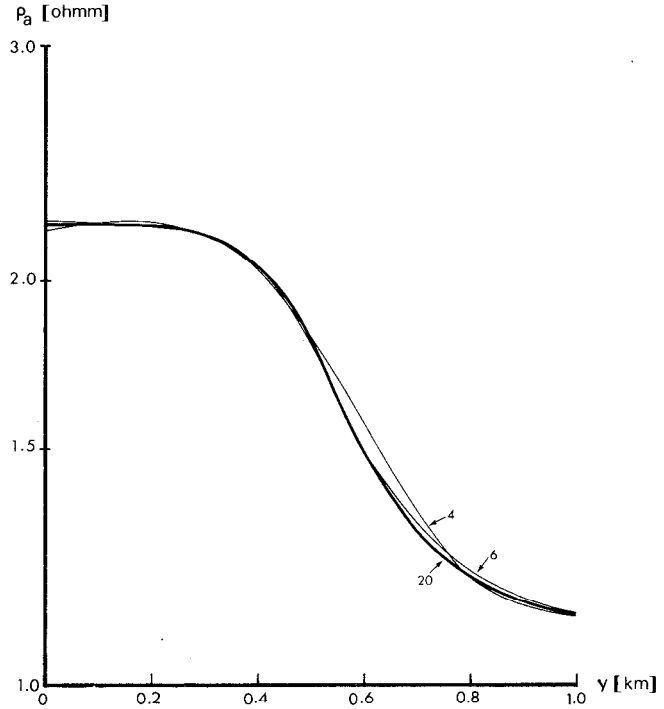

Figure 6. ρ_a-curves from the model Fig. 5. The number of coefficients is 4, 6, 20. $\omega = 2\pi$, $\rho_1 = 10$ ohmm, $\rho_2 = 1$ ohmm, $L = 0.5$ km, $h = 1.0$ km, $y_S = 1.5$ km, $d = 0.2$ km.

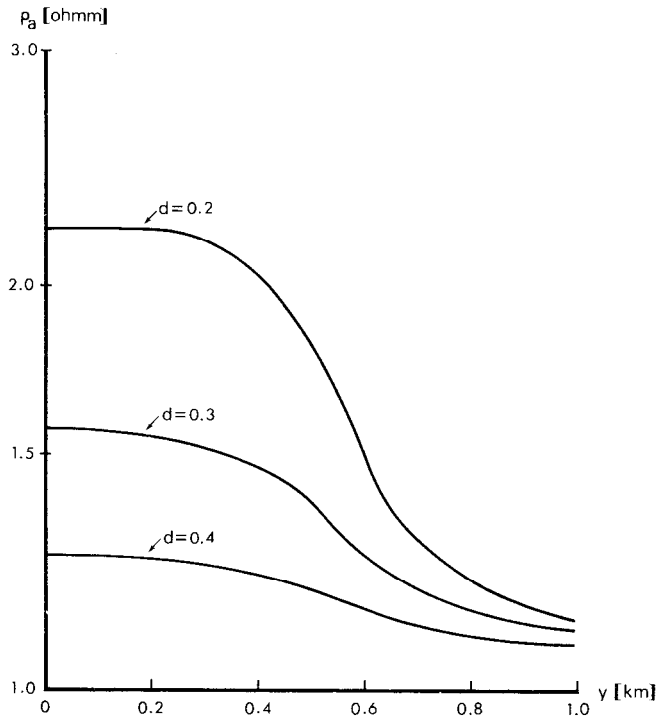

Figure 7. ρ_a-curves from the model Fig. 5. $d = 0.2$, 0.3, 0.4 km. $\omega = 2\pi$, $\rho_1 = 10$ ohmm, $\rho_2 = 1$ ohmm, $L = 0.5$ km, $h = 1.0$ km, $y_S = 1.5$ km. The number of coefficients is 10.

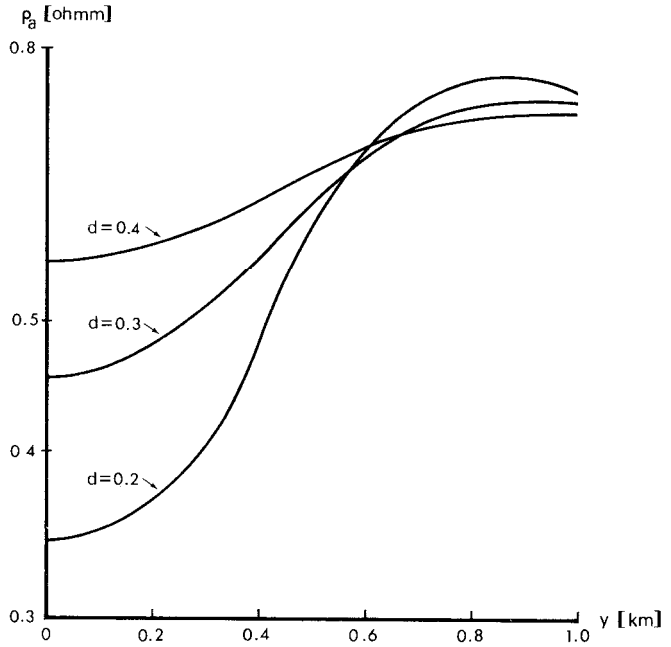

Figure 8. ρ_a-curves from the model Fig. 5. d = 0.2, 0.3, 0.4 km, $\omega = 0.2\pi$, ρ_1 = 0.1 ohmm, ρ_2 = 1 ohmm, L = 0.5 km, h = 1.0 km, y_S = 1.5 km. The number of coefficients is 10.

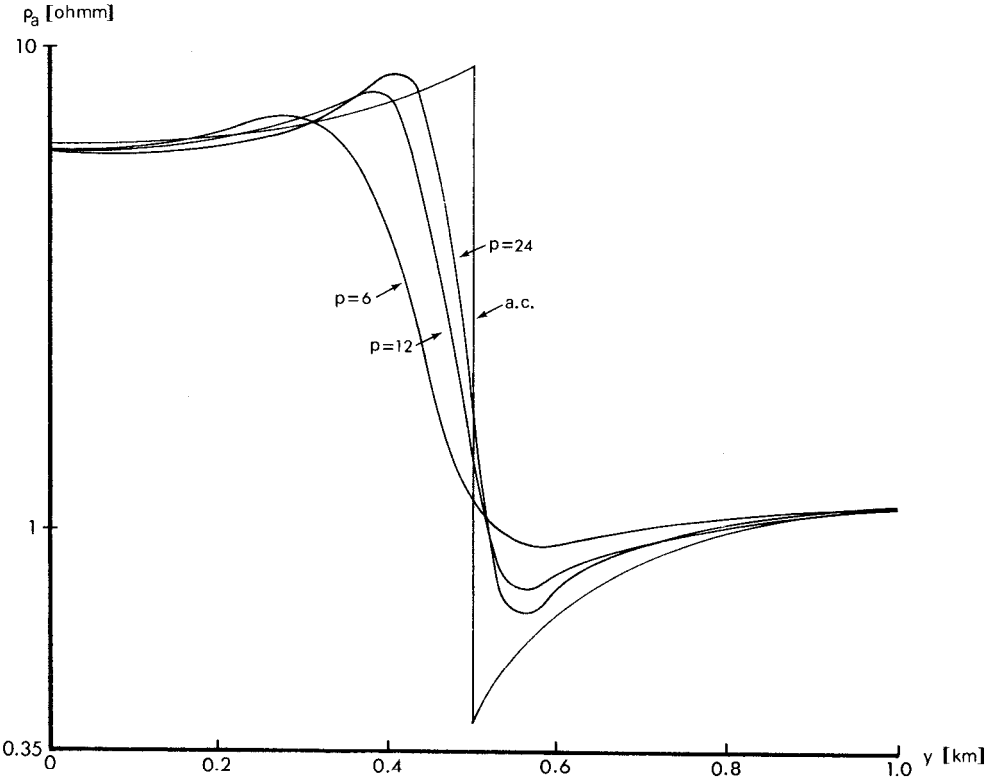

Figure 9. ρ_a-curves from the model Fig. 2 for different conductivity changes described by p = 6, 12, 18, 24. a.c. is the analytical solution to the discontinuous case. $\omega = 2\pi$, ρ_1 = 5 ohmm, ρ_2 = 1 ohmm, L = 0.5 km, y_S = 1.5 km, and the number of coefficients is 20.

interpolation, in which case the involved integrals in the z-direction can be evaluated analytically, thus requiring no surplus numerical work.

We would finally like to comment on the similarity in strength of the anomalies across good and bad conductors as shown in our examples. In the case of E-polarization there is no such similarity with the chosen examples: bad conductors will give very weak responses, whereas good conductors will give large responses.

In conclusion we may state that the present method of solving the H-polarization Integral Equation in the wavenumber domain leads to small linear systems to be solved numerically. The complicated Fourier integrals connected with the Green's tensor elements, which have to be evaluated when solving the integral equation in the space domain, are completely removed. The extension of the method to treat the E-polarization case can easily be performed, in which case only one component of the electric field is required. The method enables us to study the effect of continuous conductivity changes, in fact, formally, there is no distinction in the method between continuous and discontinuous cases.

Acknowledgments

One of us (KS) is particularly indebted to Professor J. T. Weaver for many fruitful discussions during his stay at The University of Victoria. We would also like to thank Dr P. Weidelt, The University of Göttingen, for his inspiring lectures at The University of Aarhus.

References

Bracewell, R., 1965. *The Fourier transformation and its applications,* McGraw-Hill, New York.
Coggon, J. H., 1971. *Geophys.*, **36**, 132–155.
Ghosh, D. P., 1971. *Geophysical prospecting,* **19**, 192–217.
Harrington, R. F., 1968. *Field computation by moment methods,* The Macmillan Co., New York.
Hobbs, B. A., 1975. *Phys. Earth planet. Int.*, **10**, 250–261.
Hohmann, G. W., 1971. *Geophys.*, **36**, 101–131.
Jones, F. W. & Pascoe, L. J., 1971. *Geophys. J. R. astr. Soc.*, **24**, 3–30.
La Joie, J. J., 1971. *Thesis,* Physics Department, University of Toronto, Canada.
Porstendorfer, G., 1975. *Principles of magneto-telluric prospecting,* Geopublication Associates.
Raiche, A. P., 1974. *Geophys. J.*, **36**, 363–376.
Rankin, D., 1962. *Geophys.*, **27**, 666–676.
Reddy, I. K. & Rankin, D., 1973. *Pure appl. Geophys.*, **105**, 845–857.
Weidelt, P., 1975a. *J. Geophys.*, **41**, 85–109.
Weidelt, P., 1975b. *Phys. Earth planet. Int.*, **10**, 282–291.